energies

MDPI

Article

A Fuzzy Adaptive PID Coordination Control Strategy Based on Particle Swarm Optimization for Auxiliary Power Unit

Hongyan Qin [1], Lingfeng Wang [2], Shilong Wang [2], Weitao Ruan [2] and Fachao Jiang [2,*]

[1] The School of Mechanical and Electrical Engineering, Sanjiang University, Nanjing 210012, China; qin_hongyan@sju.edu.cn
[2] College of Engineering, China Agricultural University, Beijing 100083, China; lingfengwang440@gmail.com (L.W.); wshilong@cau.edu.cn (S.W.); ruan_wt@163.com (W.R.)
* Correspondence: jfachao@cau.edu.cn

Abstract: Range extender hybrid vehicles have the advantages of better dynamics and longer driving range while reducing pollution and fuel consumption. This work focuses on the control strategy of an Auxiliary Power Unit (APU) operating in power generation mode for a range-extender mixer truck. When an operating point is switched, the engine speed and generator torque of the APU will switch accordingly. In order to ensure APU fast and stable adjustment to meet the power demand of the vehicle as well as operate at the lowest fuel consumption, a fuzzy adaptive PID coordination control strategy based on particle swarm optimization (PSO) is proposed to control the APU. The optimal operating curve of APU is calculated by coupling the engine and generator first. Then, the adaptive PID algorithm is used to control the speed and torque of the APU in a dual closed loop. The PSO is used to optimize the PID control parameter. Through hardware-in-the-loop tests under different working conditions, the control strategy is verified to be effective and real-time. The results show that the proposed control strategy can coordinate the operating of engine and generator and control the APU to track target power stably and quickly under minimum fuel consumption. Compared with traditional PID control strategy, the overshoot, regulation time and steady-state error are reduced by 55.1%, 11.1% and 77.3%, respectively.

Keywords: auxiliary power unit; adaptive; coordination control; fuzzy PID; PSO; range-extender concrete mixer truck

Citation: Qin, H.; Wang, L.; Wang, S.; Ruan, W.; Jiang, F. A Fuzzy Adaptive PID Coordination Control Strategy Based on Particle Swarm Optimization for Auxiliary Power Unit. *Energies* **2024**, *17*, 5311. https://doi.org/10.3390/en17215311

Academic Editor: Javier Contreras

Received: 30 September 2024
Revised: 21 October 2024
Accepted: 23 October 2024
Published: 25 October 2024

1. Introduction

With the rapid development of the automobile industry, the problems of energy shortage and environmental pollution become increasingly prominent [1]. Nowadays, the green revolution in the automobile industry has become a major trend. As a heavy construction vehicle, concrete mixer trucks have high fuel consumption and emissions, which is a pressing problem. An extended-range concrete mixer truck is a good solution. The extended-range concrete mixer truck has two power sources: an auxiliary power unit (APU) and battery pack [2]. The APU is composed of an engine and generator, and the engine drives the generator to generate electricity for the vehicle [3]. Since the engine operates independently of the driving conditions, it can operate stably in the optimal working area, which can save fuel while extending the range. The extended-range vehicles are widely recognized as the ideal vehicles for the transition from traditional engineering vehicles to pure engineering electric vehicles.

When the APU is in power generation mode, the improvement in fuel economy and efficiency mainly relies on the control strategy of APU [4,5]. The auxiliary power control unit (APCU) decouples the target power sent by the VCU into target speed and target torque. The engine speed is controlled by adjusting the throttle opening and the generator torque is controlled by vector control method to adjust the generator current. However, due to the highly nonlinear and strong coupling between the engine and generator in the

APU [6], in actual conditions, it is usually difficult for the APU to adjust quickly and stably to meet the power demand of the vehicle and output target power under minimum fuel consumption. The phenomena of long regulation time, large overshoot and steady-state error often occur. The dynamic response of the engine and generator are very different; therefore, the coordination control of the engine and generator to improve the dynamic performance, stability and efficiency of APU is of crucial importance.

In terms of the coordination control of APU, researchers have proposed many control strategies [7,8]. Nowadays, there are mainly two control strategies. One is to control the engine speed and the generator torque. The generator torque is the load of the engine [9–11]. The other is to control the generator speed and engine torque. The engine torque is the load of the generator. Although the second strategy outputs power faster, when the engine torque changes suddenly, the APU speed will change, which can easily cause speed fluctuation in the generator. In addition, since the current of the generator is more stable and the output torque is more accurate than that of the engine, the first strategy can reduce the vibration between engine and generator during the APU start-up phase. Therefore, we control the engine speed and the generator torque for a better control effect.

With the development and application of global optimization algorithms, some researchers have applied them to the coordination control of the APU for optimization, which has further improved the dynamic property and stability of the APU. Specifically, this has included particle swarm optimization (PSO) [12], a genetic algorithm (GA) [13,14], dynamic programming (DP) [15,16], model predictive control (MPC) [17,18], sliding mode control (SMC) [19,20] and neural network (NN) [21].

In [22], a cascade PID-based controller was established to control the speed and torque of the powertrain; the results show that the method has a high control accuracy. Taking the minimum fuel consumption as the control goal, Barsali et al. [23] used a fuzzy prediction algorithm to control the engine speed to make it operate at the optimal operating curve. Darwich et al. [24] used a PSO algorithm to solve the optimal problem of nonlinear system; the engine speed and generator torque are optimized through the global exploration ability of particle swarms to achieve efficient control of the APU.

A neural network algorithm is used to optimize the PID tuning to realize the real-time adjustment of the engine speed [25]. In order to improve the robustness and stability of the system, a sliding mode optimum control algorithm is used in the coordination control of the APU [26]. In [27], a control strategy combining fuzzy logic and adaptive optimal control was proposed to optimize the transient response of the hybrid powertrain. In [28], a strategy combining SMC technology with first-order low pass filter and adaptive PID controller was proposed, which can optimize the control parameters K_P, K_I and K_D of PID controller online in a short time. Kang et al. [29] used the MPC strategy to optimize the engine speed and generator torque online, which greatly improves the power response speed of the APU.

At present, PID controllers are mostly used in the coordinated control of the APU, but due to the strong coupling characteristics of the APU, it is difficult for a single PID control to ensure that the range extender system achieves good dynamics, stability and fuel economy. The fuzzy PID can adjust the control parameters of the PID in real time but relies excessively on the fuzzy rules. The parameters of the fuzzy controller remain unchanged and optimal control cannot be achieved. Therefore, we adaptively optimize fuzzy control parameters by PSO to improve the stability and robustness of the system. According to the working status of the APU, the PID control parameters are adjusted in real time to improve the system adjustment speed and steady-state accuracy, and reduce the amount of overshoot. In this work, the APU power tracking control strategy is proposed. The strategy uses a fuzzy PID algorithm for dual closed-loop control of engine speed and generator torque, and the PSO algorithm is utilized to correct the PID tuning parameters. To minimize fuel consumption, the APU fuel consumption characteristics map is obtained through coupling, and the engine fuel consumption map and generator efficiency map are calculated. Further, the optimal operating curve is also obtained. The target power is

decoupled into target engine speed and target generator torque according to the optimal operating curve of APU. The strategy controls APU tracking target power by adjusting the engine speed and generator torque to a certain target value in a dual closed loop. Through the fuzzy adaptive PID algorithm based on PSO, the engine speed and generator torque are adjusted to the target values. As a result, the APU responds to the target power more quickly, accurately and stably. Finally, a hardware in the loop (HIL) test platform is built to verify the effectiveness and reliability of the control strategy. The proposed control strategy has good application prospects in efficient and stable control of the APU.

2. Models and Methods

2.1. Powertrain and System Configuration

The powertrain model of the extended-range concrete mixer truck is shown in Figure 1. The extended-range concrete mixer truck is mainly composed of the power battery pack, APU, drive motor, gearbox, hydraulic transmission system, reducer and mixing drum. Compared to hybrid vehicles, extended-range concrete mixer trucks have two power consumption units—drive motor and mixing drum [30,31]—which makes the powertrain more complex. There are two power sources in the extended-range concrete mixer truck: the battery pack as the main power source and the APU as the auxiliary power source. When the vehicle is operating, the battery pack and the APU together provide the energy required by the drive motor and the mixing drum. The APU is composed of engine, integrated starter and generator (ISG) and clutch. The engine is a diesel engine with good power and reliability and the ISG is a three-phase permanent magnet synchronous motor (PMSM). The configuration of the engine and ISG is shown in Tables 1 and 2.

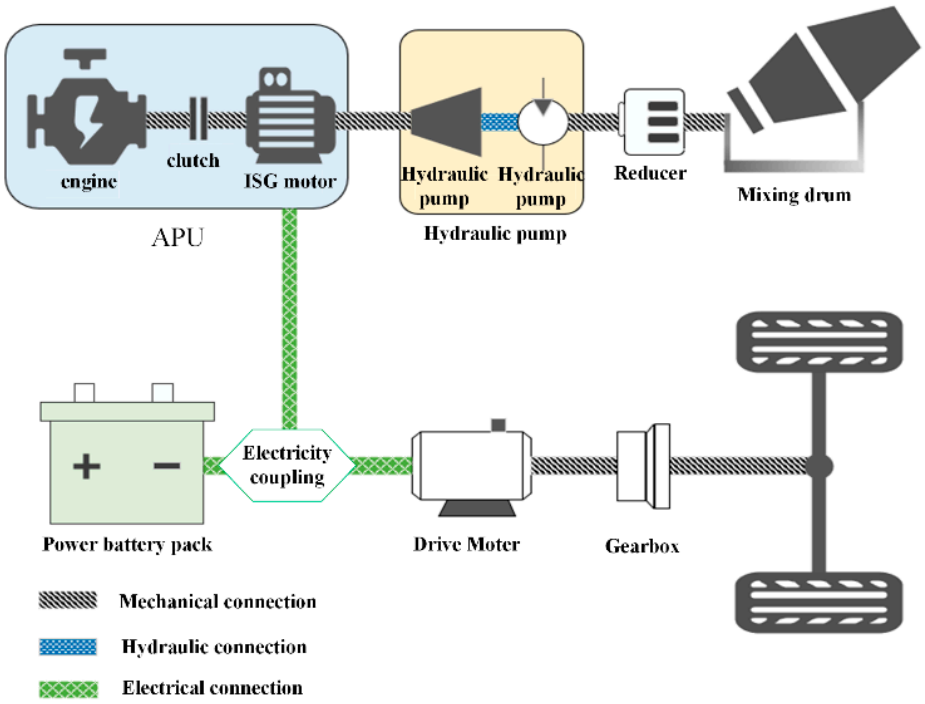

Figure 1. Powertrain of extended-range concrete mixer truck.

As Figure 2 shows, the architecture of the whole vehicle's control system is multi-layer and distributed. The top layer is the VCU, which is the core of the control system. The middle layer includes a battery management system (BMS), APCU and others, and receives the command signals from the VCU, coordinates the internal operation of each subsystem, and feeds back the status signals of each subsystem in real time. The bottom layer is the control units of actuators, which are also the controllers closest to the mechanical components, mainly including the engine control unit (ECU), ISG control unit (GCU) and

clutch control unit (CCU). The function of the bottom layer is to receive the signals from the middle layer controllers and control the operating states of the actuators. Data are transmitted via CAN bus.

Table 1. Configuration of engine.

Engine	ISF 3.8 Four-Stroke High-Speed Diesel Engine
Number of cylinders	4
Engine displacement (L)	3.76
Rated speed (rpm)	2600
Maximum torque speed	1200–1900
Maximum output power (kW)	125
Maximum output torque (Nm)	450–600

Table 2. Configuration of ISG.

Generator	YQW3-225Z-18A-RA2
Rated power (kW)	80
Rated torque (N·m)	425
Rated speed (rpm)	1800
Peak power (kW)	130
Maximum speed (rpm)	3000
Rated current (A)	119
Number of pole pairs of the motor	6

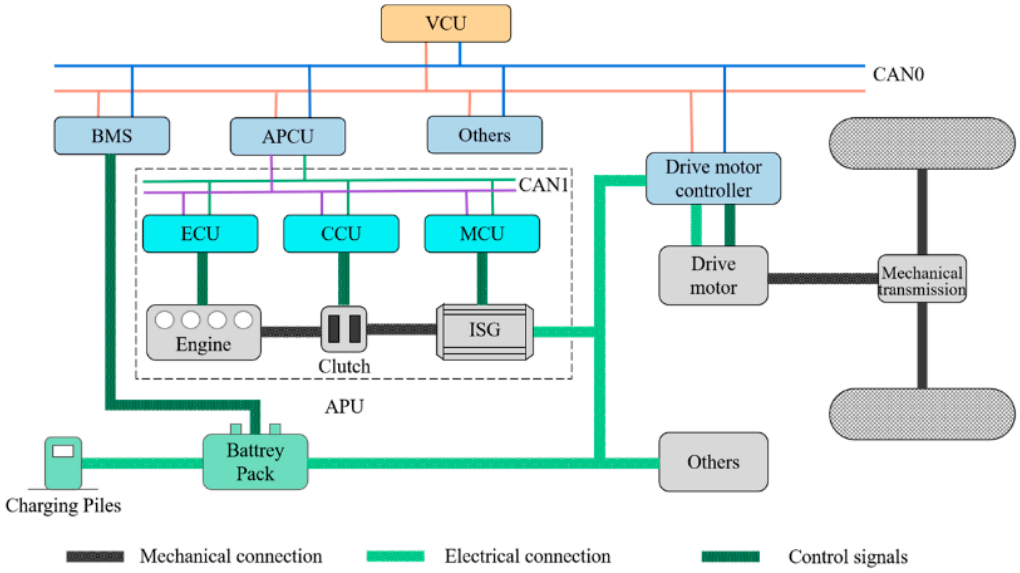

Figure 2. Architecture of the whole vehicle's control system.

This study mainly focuses on the control strategy of the APU. After receiving the commands from the VCU, the APCU controls the start and stop of the engine, clutch and ISG. The APCU decouples the target power into target engine speed and target ISG torque along the optimal operating curve. The signals of target engine speed and target ISG torque are transferred to the ECU and GCU, then the engine and ISG respond to the control commands from the APCU and provide feedback on the state signals in real time. The dual closed-loop control strategy controls the engine and ISG through the fuzzy adaptive PID algorithm based on PSO to adjust the actual output power to be closer to the target power.

2.2. Selection of APU Operating Point

The operating point of the APU affects the dynamics and economy property, which should not only satisfy the power demand of the whole vehicle, but also ensure the APU

operates at the lowest fuel consumption. Since the APU is composed of an engine and ISG, we can get APU fuel consumption characteristics map based on engine fuel consumption map and ISG efficiency map.

1. Engine Model

According to the experimental data of the engine, the engine fuel consumption map is expressed as shown in Figure 3. The full load speed characteristics curve indicates the maximum torque corresponding to different engine speeds at maximum power.

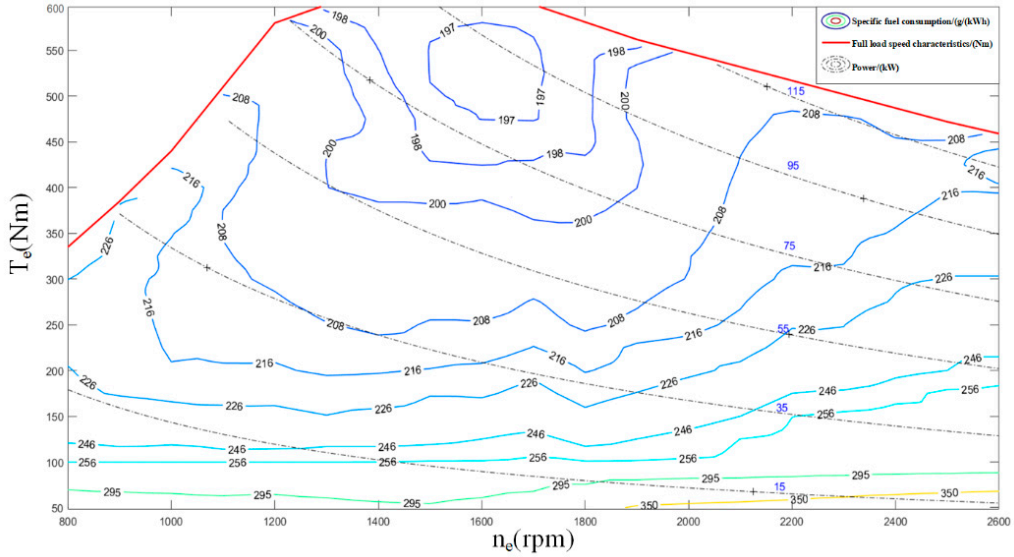

Figure 3. Engine fuel consumption map.

2. ISG Model

According to the experimental data of ISG, the ISG efficiency map is expressed as shown in Figure 4. Figure 4 is divided into two parts according to the positive and negative torque. In the upper part, ISG operates at the electric mode and in the lower part it operates at the power generation mode. The full load speed characteristics curve indicates the maximum torque corresponding to different ISG speeds at maximum power.

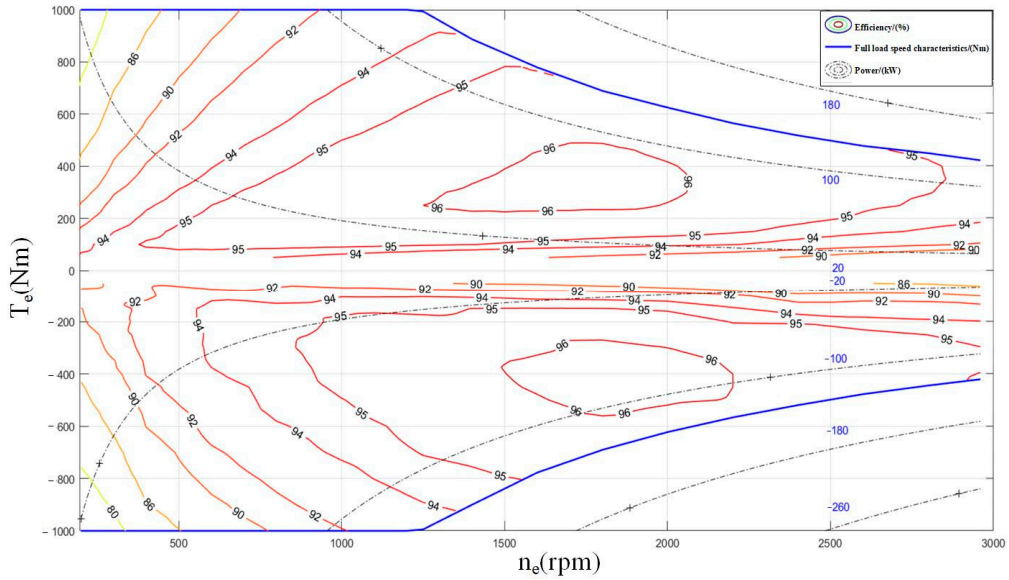

Figure 4. ISG efficiency map.

3. APU Model

During the steady-state power generation mode, the clutch is fully engaged, and the engine and the ISG share the same speed. At that speed, the corresponding operating efficiency and actual torque of the ISG can be calculated. The APU output power can be calculated by (1).

$$P_{APU} = P_e \times \eta_{ISG} \quad (1)$$

where η_{ISG} is the operating efficiency of ISG, P_{APU} is the output power of APU and P_e is the output power of engine.

The APU fuel consumption characteristics map can be coupled with the engine and ISG characteristics, as shown in Figure 5. By using the ergodic optimization algorithm, the optimal operating point which ensures engine operating at the minimum fuel consumption for each power can be found. Connect these points to form the optimal operating curve of the APU. When the target power is known, we decouple the target power into target engine speed and target ISG torque along the optimal operating curve. The signals of target speed and torque are transferred to ECU and GCU, respectively, for tracking control. The actual output power of the APU can be expressed as (2).

$$P_{APU} = N_e \times T_{ISG}/9550 \quad (2)$$

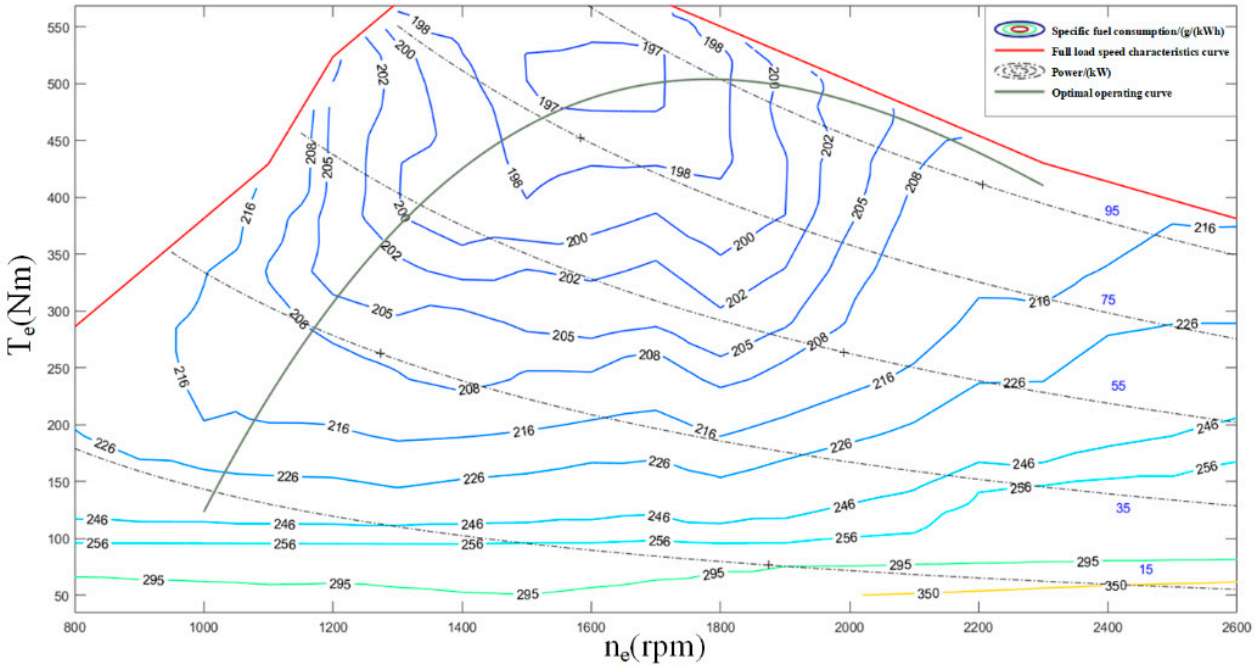

Figure 5. APU fuel consumption characteristics map and the optimal operating curve.

3. Power Control Strategy for APU

3.1. Fuzzy PID Control Strategy

The coordinated control strategy of APU is shown in Figure 6. Firstly, the target generation power is determined, and then the target power is decoupled into target speed and target torque according to the optimal fuel consumption curve of the APU. The engine and ISG are controlled by control algorithm in a dual closed loop, respectively. This strategy provides dual closed-loop control of the engine and ISG to achieve a fast and stable response of speed and torque to target values. For the dual closed-loop algorithm, the difference between engine target and actual speed and ISG target and actual torque are the inputs and the actual speed and torque are the outputs.

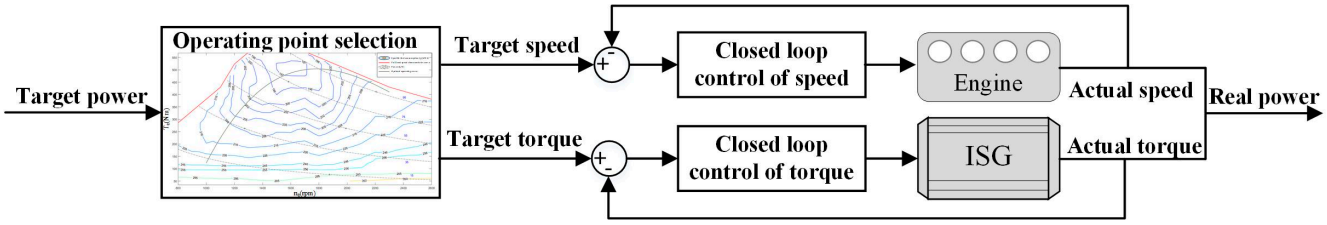

Figure 6. Dual closed-loop coordinated control strategy of APU.

4. Incremental PID

Dual closed-loop control for speed and torque is the basis of coordinated control strategy. Control of speed and torque can be tracked using a PID algorithm.

The discrete expression of the PID algorithm is as (3).

$$u(k) = K_P e(k) + K_I \sum_{j=0}^{k} e(k)T + K_D[e(k) - e(k-1)]/T \tag{3}$$

where $e(k)$ is the difference between the target and actual value at moment k. $u(k)$ is the output control quantity. T is the sampling period. K_P is the proportional gain. K_I is the integral gain and K_D is the derivative gain.

In order to obtain better control stability, we use the incremental PID control algorithm with the calculation (4). The differences between the target speed/torque and actual speed/torque values are used as inputs, and the incremental PID algorithm regulates the engine throttle opening and the current of the ISG to control speed/torque.

$$\Delta u(k) = K_P[e(k) - e(k-1)] + K_I e(k) + K_D[e(k) - 2e(k-1) + e(k-2)] \tag{4}$$

where $\Delta u(k)$ denotes the rate of change of the control quantity.

5. Fuzzy PID

The traditional incremental PID control algorithm can achieve power tracking, but its steady-state and transient performance is still poor. Fuzzy PID is the combination of fuzzy control and PID control, which has the advantage of strong stability. To achieve a fast and stable tracking to the target power and improve APU efficiency, we utilize fuzzy PID algorithm for dual closed-loop control of speed and torque. As Figure 7 shows, the error E and the differential error dE/dt of the engine speed and ISG torque are inputs, and through inference and calculation of the fuzzy logic controller (FLC), the correction coefficients ΔK_P, ΔK_I and ΔK_D are outputs to the PID controller for adjustment of PID parameters. In Figure 7, K_E and K_{Ec} are quantification factors of the error and differential error, respectively. K_U is the scale factor.

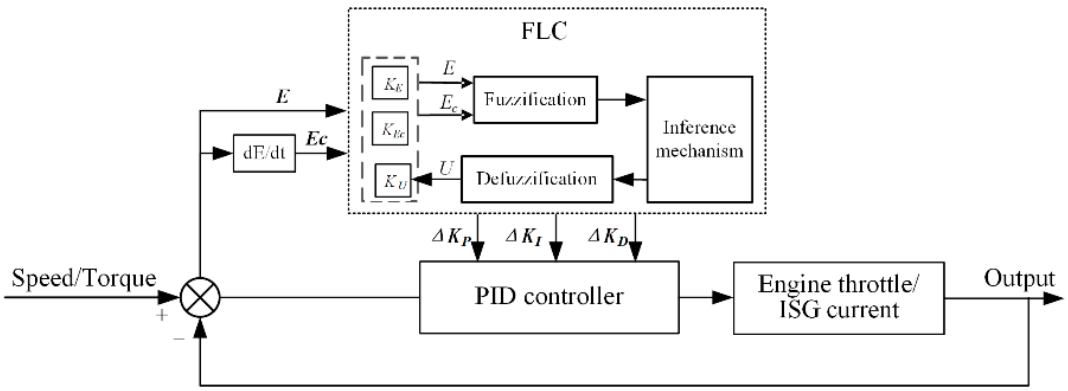

Figure 7. Schematic of fuzzy PID control algorithm.

The inputs of the FLC are E and dE/dt of speed/torque and the outputs are correction coefficients ΔK_P, ΔK_I and ΔK_D. Considering that the fuzzy PID controller has 2 inputs, the two-dimensional FLC is used. The continuous variables of inputs are converted to fuzzy variables in the discrete universe by (5):

$$\varepsilon_a = [\varepsilon - (a+b)/2] \times 2n/(b-a) \tag{5}$$

where ε is the input variables in continuous interval, $\varepsilon \in [a, b]$; ε_a is the corresponding fuzzy value of ε in the discrete universe of discourse, $\varepsilon_a \in [-n, n]$.

Variables are divided into seven linguistic labels: negative big (NB), negative medium (NM), negative small (NS), zero (ZE), positive small (PS), positive medium (PM) and positive big (PB). In order to achieve a fast response time, while taking into account a large range of variations in engine speed and ISG motor torque, membership functions (MFs) are a combination of triangles and bilateral Gaussian functions. The MFs of inputs and outputs are shown in Figure 8.

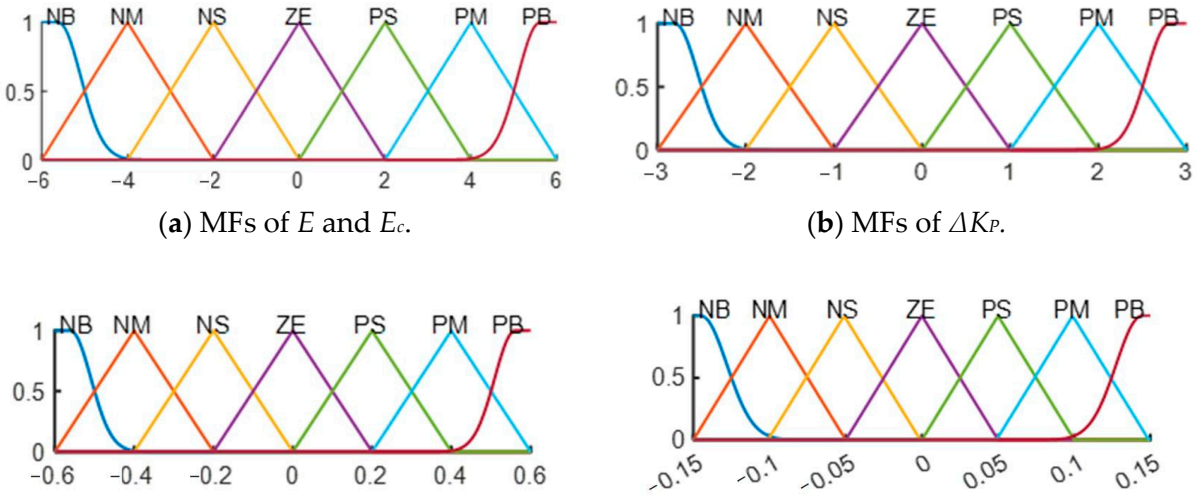

(**a**) MFs of E and E_c.

(**b**) MFs of ΔK_P.

(**c**) MFs of ΔK_I.

(**d**) MFs of ΔK_D.

Figure 8. MFs of inputs and outputs.

Fuzzy rules are the core of FLC. According to the role of control parameters in the system, we designed the fuzzy rules for ΔK_P, ΔK_I and ΔK_D, as shown in Tables 3–5. The fuzzy rules surfaces are shown in Figure 9.

Table 3. Fuzzy rule for ΔK_P.

E \ E_c	NB	NM	NS	ZE	PS	PM	PB
NB	PB	PB	PM	PM	PM	PS	ZE
NM	PB	PB	PB	NM	PM	ZE	ZE
NS	PM	PM	PM	PS	ZE	NB	NM
ZE	PM	PS	PS	ZE	NS	NS	NM
PS	NM	NB	NB	NB	PS	PM	PM
PM	NB	NM	NM	PM	PM	PM	PB
PB	NB	NB	NM	NM	PM	PB	PB

Table 4. Fuzzy rule for ΔK_I.

E \ E_c	NB	NM	NS	ZE	PS	PM	PB
NB	NB	NB	NB	NM	NM	ZE	ZE
NM	NB	NB	NM	NM	NS	ZE	ZE
NS	NM	NM	NS	NS	ZE	PS	PS
ZE	NM	NS	NS	ZE	PS	PS	PM
PS	NS	NS	ZE	PS	PS	PM	PM
PM	ZE	ZE	PM	PM	PM	PM	PB
PB	ZE	NS	PS	PM	PB	PB	PB

Table 5. Fuzzy rule for ΔK_D.

E \ E_c	NB	NM	NS	ZE	PS	PM	PB
NB	NB	NB	NB	ZE	ZE	PS	PS
NM	NB	NB	NB	ZE	ZE	PS	PS
NS	NB	ZE	ZE	ZE	ZE	PS	PS
ZE	ZE	ZE	ZE	ZE	ZE	ZE	ZE
PS	NB	NB	ZE	ZE	ZE	PS	PS
PM	NB	NB	NB	ZE	ZE	PS	PS
PB	NB	NB	NB	ZE	ZE	PS	PS

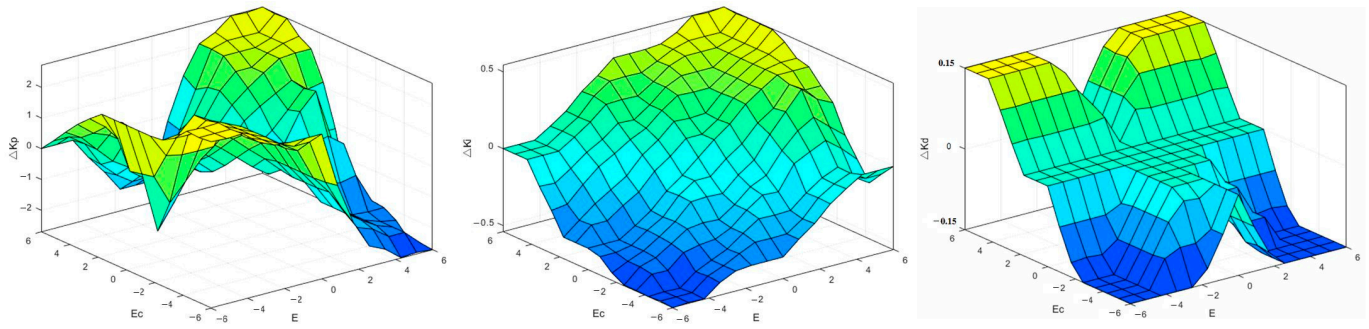

(**a**) Fuzzy rule surface of ΔK_P. (**b**) Fuzzy rule surface of ΔK_I. (**c**) Fuzzy rule surface of ΔK_D.

Figure 9. Fuzzy rule surfaces.

Finally, defuzzification is carried out by the weighted average method to convert the fuzzy quantities obtained by the fuzzy rules into the corresponding numerical data. The formula is

$$Y = \sum_{i=1}^{n} w_i Y_i / \sum_{i=1}^{n} w_i \tag{6}$$

where Y refers to the final output; Y_i is the output elements; w_i is the membership function value of Y_i.

3.2. Fuzzy Adaptive PID Coordination Control Strategy Based on PSO

The fuzzy PID can adjust the control parameters of the PID in real time, but relies excessively on the fuzzy rules. The parameters of the fuzzy controller remain unchanged and optimal control cannot be achieved. Therefore, we adaptively optimize fuzzy control parameters by PSO to improve the stability and robustness of the system. Based on the analysis above, we propose a fuzzy adaptive PID coordination control strategy based on PSO.

1. Particle Swarm Optimization Algorithm

PSO is a swarm intelligent optimization algorithm developed by Eberhart and Kennedy based on the foraging behavior of animals. First, the velocity and position of particles are randomly initialized. Then, through an iterative search, the motion state of each particle is updated and the search range is continuously converged. At the end of the iterative search, the optimal value is obtained [32]. The velocity and position of each particle in the PSO algorithm can be expressed as

$$\begin{cases} v_{k+1} = wv_k + c_1r_1(pb_k - x_k) + c_2r_2(gb_k - x_k) \\ x_{k+1} = x_k + v_{k+1} \end{cases} \tag{7}$$

where w is the inertia weight, which determines the inheritance degree of the current velocity to the previous velocity of the particle; v_k is the current velocity vector of the particle; x_k is the current position of the particle; c_1 and c_2 are both learning rates, which represent the attraction intensity of the individual optimal solution and group optimal solution to the particle, respectively. pb_k represents the best historical position of the particle and gb_k represents the global best position of the particle swarm by current iteration. r_1 and r_2 are random numbers between [0,1].

In order to solve the disadvantage that the parameters of fuzzy control cannot be adjusted adaptively, this paper uses the PSO algorithm to optimize the quantization factors K_E, K_{Ec} and scale factor K_U of the fuzzy PID controller. Taking Integral of Time and Absolute Error (ITAE) as the evaluation index, the fitness function is as follows [33,34]:

$$J = \int_0^\infty t|e|dt \tag{8}$$

where J is evaluation index, t represents time and e is error.

Figure 10 shows the schematic of fuzzy PID control based on PSO. Using E and E_c of speed/torque as the inputs, K_E, K_{Ec} and K_U are optimized through the PSO algorithm. Find the factor with the highest level fitness and optimize E, E_c and correction coefficients ΔK_P, ΔK_I and ΔK_D of PID parameters to realize the adaptive control of speed and torque.

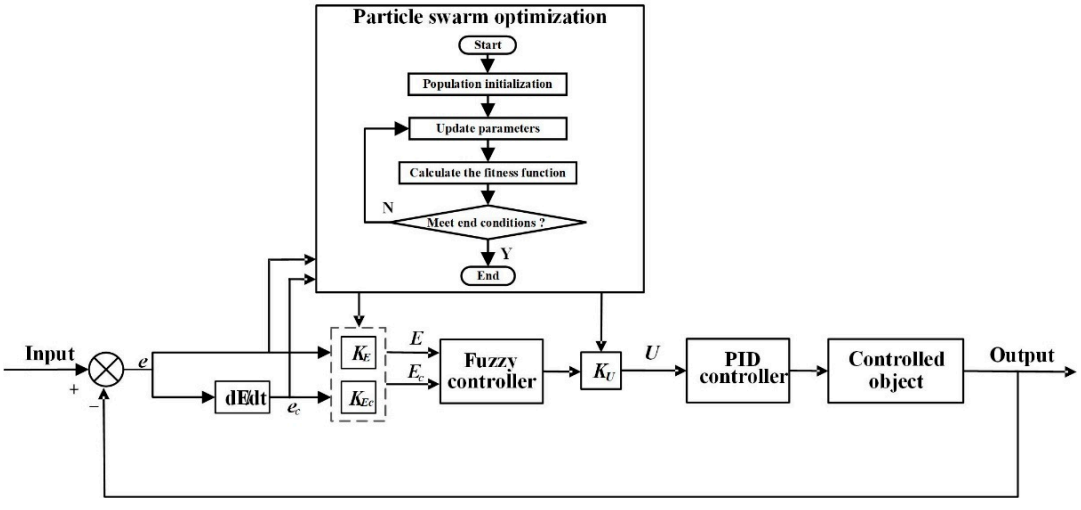

Figure 10. Schematic of fuzzy PID control based on PSO.

Writing PSO algorithm in MATLAB (R2021a) and joint simulation with fuzzy PID controller model in Matlab/Simulink (R2021a). The number of particles is set to 20. w = 0.6. The maximum number of iterations is 100, and the learning rates $c_1 = c_2 = 2$. The fitness function curves of the controller for speed and torque are shown in Figure 11. From Figure 11, we know that the fitness function value of the speed obtains the optimal solution at the 39th iteration, with the value of 1.293. The optimized parameters are as follows:

E = 3.5, E_c = 0.75, ΔK_P = 11.8103, ΔK_I = 0.1833, ΔK_D = 0.0558; the fitness function value of the torque obtains the optimal solution at the 35th iteration, with the value of 1.162. The optimized parameters are as follows: E = 1.5, E_c = 0.2, ΔK_P = 2.0225, ΔK_I = 0.2334, ΔK_D = 0.1065.

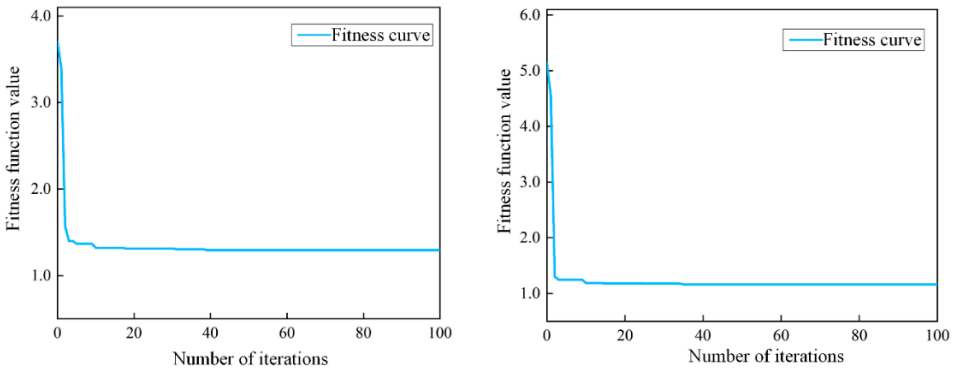

(**a**) Fitness curve of speed. (**b**) Fitness curve of torque.

Figure 11. Fitness function values of speed and torque.

2. Fuzzy adaptive PID coordination control strategy based on PSO

The strategy structure is presented in Figure 12. The VCU allocates the energy reasonably and calculates the generating power required by the APU according to the actual driving conditions. The APCU decouples the target power into engine target speed and ISG target torque based on the optimal operating curve. The control module receives the target and actual values of engine speed and ISG torque and calculates the error and differential error. The PSO algorithm takes E and the dE/dt as inputs. K_E, K_{Ec} and K_U are iterative-optimized by PSO. Taking ITAE as the judgment standard, the factor with the highest level of fitness is found and the optimal combination of K_E, K_{Ec} and K_U are obtained. At the same time, the FLC infers and outputs factors according to the knowledge base. K_U is used to optimize the factors to obtain the correction coefficients ΔK_P, ΔK_I and ΔK_D. Then, the control parameters K_P, K_I and K_D of the PID controller with optimal performance under this operating condition are obtained. The PID controller with optimized control parameters can control the engine speed and ISG torque in real time and adaptively.

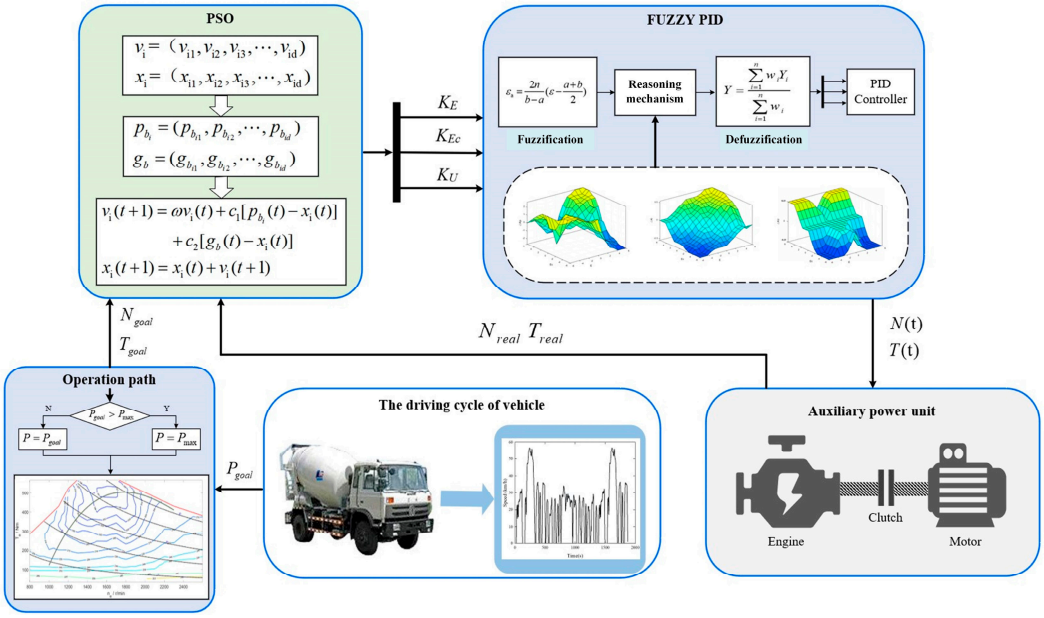

Figure 12. Fuzzy adaptive PID coordination control strategy based on PSO.

4. Experiment and Analysis

In this section, the effectiveness and real-time performance of the control strategy are verified through an HIL test. The power response characteristic test of the coordination control strategy is completed at various working conditions. The PID control strategy, fuzzy PID control strategy and fuzzy adaptive PID coordination control strategy based on PSO are all tested and compared, and the test results are statistically analyzed.

4.1. HIL Test Platform

The HIL test platform is shown in Figure 13. It mainly consists of the real-time system, upper computer software and APU controller. The chip of APU controller is XC2267M, manufactured by Infineon in Munich, Germany. Connect the actual controller to the simulation platform. The real-time system simulates the operation state of the APU and the signals are transferred among the upper computer, controller and real-time system through a CAN bus. The HIL system runtime is synchronized with real time, so it can accurately reflect the control effect of the control strategy.

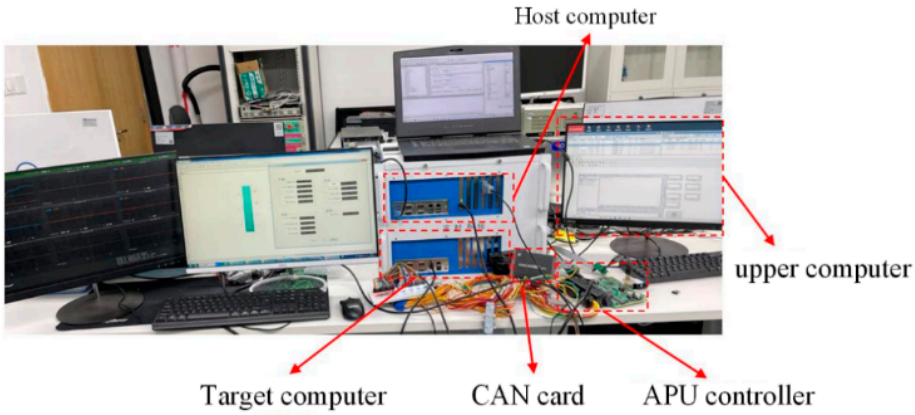

Figure 13. HIL test platform.

We build a real-time system based on xPC-Target environment, which operates in "dual-computer mode". The real time system is composed of the target computer and the host computer. The target computer is composed of a processor, CAN communication board, analog resistance board, etc., which is used to carry the powertrain model of the APU and drive the program code. The host computer is responsible for building the model and monitoring the status of the target computer. The function configuration of the main ports of the real-time system is shown in Table 6.

Table 6. Main ports configuration of real time system.

Name	Number	Range
Bidirectional PWM	4	0–5 V/0–24 V
PWM signal output	10	0–5 V/0–24 V
Hall signal acquisition	10	0–5 V/0–24 V
High effective digital signal output	32	5–24 V
Low effective digital signal output	32	
Analog signal output	12	0–5 V
Analog signal acquisition	32	0–5 V/0–12 V/0–24 V Configurable
CAN communication node	12	
High-side driven load	10	
Low-side driven load	20	
Fault injection port	100	

4.2. HIL Test

The HIL system adopts a real controller, which can restore real computing environment and sampling time. In order to verify the feasibility and real-time performance of the proposed fuzzy adaptive PID coordination control strategy based on PSO, power response tests under different working conditions are carried out on the HIL test system.

The target power variation for simulation testing is set as 0–1–3–6–10–15–21–28–36–45–55 kW to study the power response at power transitional conditions. The target power increments of this working condition are 1–2–3–4–5–6–7–8–9–10 kW per second. As Figure 14 shows, when the target power is small, the APU responds quickly and it can control the engine and ISG to execute the corresponding commands in time. With the increase in the amount of power change per unit time, the power regulation time gradually increases, but the overshoot and steady-state error are both within 1 kW. During the test, when the regulation time is less than 1 s, the power tracking effect can be achieved.

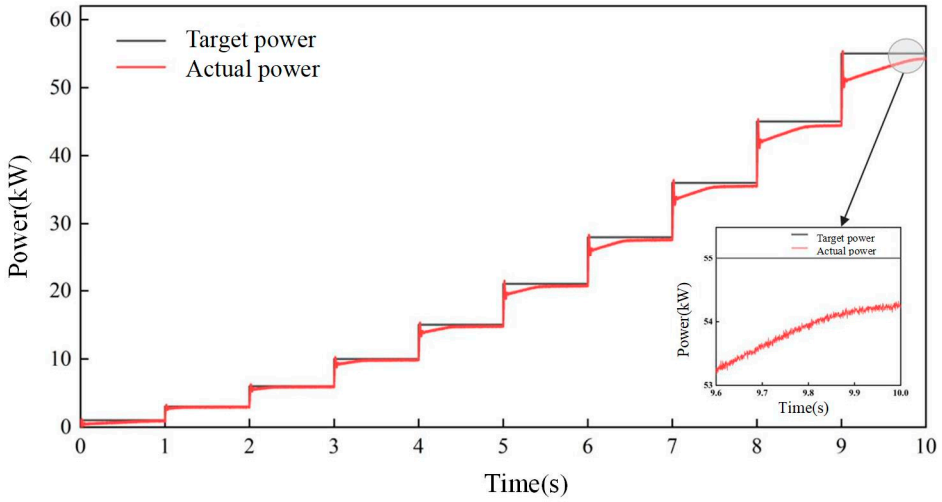

Figure 14. Power response of HIL test.

In order to further verify the power tracking effect of the control strategy when the operating point is switched, we use three working conditions for the HIL test, as Table 7 shows.

Table 7. Working conditions for HIL test.

Working Conditions	Target Power (kW)	Power Increment Change (kW/s)
1	0–1–3–6–10–15–21–28–36–45–55	1–2–3–4–5–6–7–8–9–10
2	0–2–6–12–20–30–38–44–48–50	2–4–6–8–10–8–6–4–2
3	0–10–20–30–40–50–60–70–80–90	10–10–10–10–10–10–10–10–10

For the APCU, the response effect of target power is mainly evaluated by the performance index such as overshoot, regulation time and steady-state error at transitional conditions. In this paper, taking power transition from 45 kW to 55 kW in working condition 1, power transition from 20 kW to 30 kW in working condition 2 and power transition from 50 kW to 60 kW in working condition 3 as transitional conditions, the control strategy is validated. The target power for all these three transition conditions is 10 kW per second, and these three transition conditions cover multiple typical power variation intervals, so the control strategy can be validated comprehensively.

Figure 15 is the HIL test results. From Figure 15, we can see that in the early adjustment stage, the PID control strategy has the phenomenon of oscillation and the largest steady-state error, but it can still meet the power demand. Combined with the test data in Table 8, we know that the fuzzy PID control strategy has obvious improvement in terms of overshoot

and steady-state error compared with traditional PID control strategy, but the regulation time is relatively increased. The fuzzy adaptive PID coordination control strategy based on PSO has the steady-state power closest to the target power as well as the minimal adjustment time and overshoot. The fuzzy adaptive PID coordination control strategy based on PSO has the best control effect. Compared with the PID control strategy, the overshoot, regulation time and steady-state error of the fuzzy adaptive PID coordination control strategy based on PSO are reduced by 55.1%, 11.1% and 77.3%, respectively, which has the best control effect.

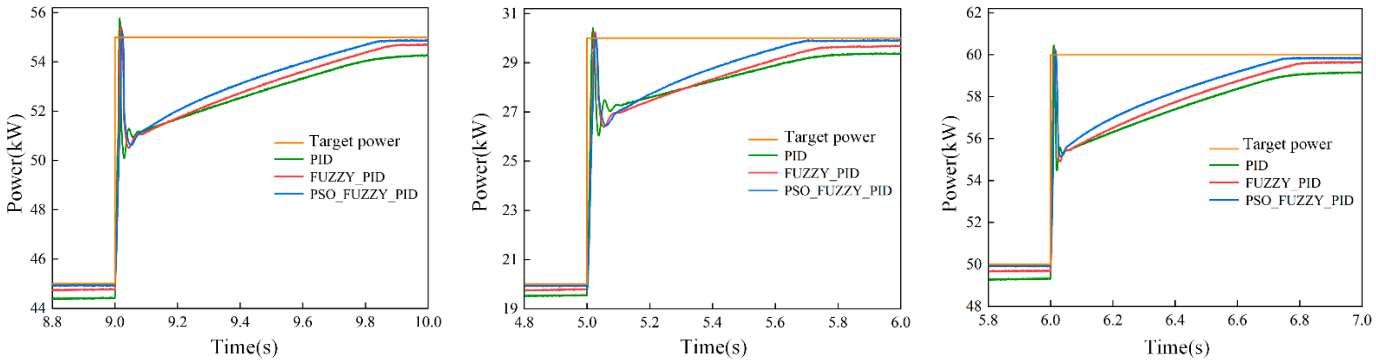

Figure 15. Target power tracking effect of three control strategies under different transitional conditions: (**a**) 45–55 kW in working condition 1; (**b**) 20–30 kW in working condition 2; (**c**) 50–60 kW in working condition 3.

Table 8. HIL test results of different control strategies.

Condition	Control Algorithm	Overshoot (kW)	Regulation Time (s)	Steady-State Error (kW)
45–55 kW	PID	0.34	0.86	0.76
	FUZZY_PID	0.20	0.94	0.33
	PSO_FUZZY_PID	0.15	0.80	0.18
20–30 kW	PID	0.42	0.84	0.70
	FUZZY_PID	0.27	0.93	0.41
	PSO_FUZZY_PID	0.19	0.75	0.12
50–60 kW	PID	0.46	0.90	0.79
	FUZZY_PID	0.31	0.99	0.36
	PSO_FUZZY_PID	0.21	0.85	0.21

The HIL test results indicate that the fuzzy adaptive PID coordination control strategy based on PSO has the best power response effect and control performance, which can effectively reduce the overshoot, regulation time and steady-state error. The proposed control strategy can not only coordinate the control engine and ISG, but also improve the power response speed and stability of APU on the basis of operating at minimum fuel consumption. Regular methods require frequent parameter adjustments to adapt to environmental variations, which is cumbersome. Meanwhile, the proposed PSO_FUZZY_PID can adaptively regulate the parameters, which enables it to be better applied in various operation scenarios.

5. Conclusions

In this paper, three speed-torque adjustment modes are proposed for the control of engine speed and ISG motor torque, and the control performance of simultaneous speed and torque adjustment is proved to be the best through simulation verification. On this basis, the FUZZY_PID and PSO_FUZZY_PID control algorithms are designed to optimize

and adjust the control parameters of the system in real time, which have good simulation results. A fuzzy adaptive PID coordination control strategy based on PSO was proposed. HIL test results show that the proposed control strategy can coordinate the operation of the engine and ISG. The strategy can make the APU output the target power quickly and accurately by controlling the engine speed and ISG torque in a dual closed loop. Moreover, it can control the APU to generate power efficiently and stably on the basis of operating at minimum fuel consumption. Compared with PID control strategy, the fuzzy adaptive PID coordination control strategy based on PSO has a 55.1% decrease in power overshoot, 11.1% decrease in regulation time and 77.3% decrease in steady-state error.

The developed range extender control system and control strategy are carried out on the simulation platform, and the follow-up work will be tested on the bench and the real vehicle to further verify its effectiveness and feasibility.

Author Contributions: Conceptualization, H.Q. and L.W.; Methodology, F.J.; Software, H.Q. and L.W.; Validation, W.R.; Formal analysis, S.W.; Investigation, W.R.; Data curation, H.Q. and L.W.; Writing—original draft, S.W.; Writing—review & editing, F.J.; Project administration, H.Q. and L.W. All authors have read and agreed to the published version of the manuscript.

Funding: This work is supported by the National Key Research and Development Program of China [Grant No. 2022YFD2001204].

Data Availability Statement: Data available on request due to privacy restrictions. The data presented in this study are available on request from the corresponding author.

Acknowledgments: The author would like to acknowledge the support of the Fengzhi Ruilian Technologies Co. Ltd. of Beijing, China.

Conflicts of Interest: The authors declare no conflict of interest.

References

1. Chen, H.; Ding, M.; Li, Y.; Xu, H.; Li, Y.; Wei, Z. Feedstocks, environmental effects and development suggestions for biodiesel in China. *J. Traffic Transp. Eng.* **2020**, *7*, 791–807. [CrossRef]
2. Verma, S.; Mishra, S.; Gaur, M.; Chowdhury, S.; Mohapatra, S.; Dwivedi, G.; Verma, P. A comprehensive review on energy storage in hybrid electric vehicle. *J. Traffic Transp. Eng.* **2021**, *8*, 621–637. [CrossRef]
3. Chen, B.; Wu, Y.; Tsai, H. Design and analysis of power management strategy for range extended electric vehicle using dynamic programing. *Appl. Energy* **2014**, *113*, 1764–1774. [CrossRef]
4. Lan, S.; Stobart, R.; Chen, R. Performance comparison of a thermoelectric generator applied in conventional vehicles and extended-range electric vehicles. *Energy Convers. Manag.* **2022**, *266*, 115791. [CrossRef]
5. Xiao, B.; Walker, P.D.; Zhou, S.; Yang, W.; Zhang, N. A Power Consumption and Total Cost of Ownership Analysis of Extended Range System for a Logistics Van. *IEEE Trans. Transp. Electrif.* **2022**, *8*, 72–81. [CrossRef]
6. Xu, Y.; Zhang, H.; Yang, Y.; Zhang, J.; Yang, F.; Yan, D.; Yang, H.; Wang, Y. Optimization of energy management strategy for extended range electric vehicles using multi-island genetic algorithm. *J. Energy Storage* **2023**, *61*, 106802. [CrossRef]
7. Zhang, H.; Yang, Q.; Song, J.; Fu, L. Study and Realization on Power Energy Distribution Control for Auxiliary Power Unit. *Energy Procedia* **2017**, *105*, 2601–2606. [CrossRef]
8. Sun, G.; Sun, D.; Ma, K.; Kan, Y.; Shi, J. Analysis and control of engine starting process based on a novel single-motor power-reflux hybrid electric vehicle. *Mech. Mach. Theory* **2022**, *168*, 104616. [CrossRef]
9. Li, J.; Wang, Y.; Chen, J.; Zhang, X. Study on energy management strategy and dynamic modeling for auxiliary power units in range-extended electric vehicles. *Appl. Energy* **2017**, *194*, 363–375. [CrossRef]
10. Wang, J.; Cai, Y.; Chen, L.; Shi, D.; Wang, R.; Zhu, Z. Review on multi-power sources dynamic coordinated control of hybrid electric vehicle during driving mode transition process. *Int. J. Energy Res.* **2020**, *44*, 6128–6148. [CrossRef]
11. Xu, D.; Zhang, J.; Zhou, B.; Yu, H. Investigation of mode transition coordination for power-split hybrid vehicles using dynamic surface control. *Proc. Inst. Mech. Eng. Part K J. Multi-Body Dyn.* **2019**, *233*, 696–713. [CrossRef]
12. Wang, Y.; Shen, Y.; Yuan, X.; Yang, Y. Operating Point Optimization of Auxiliary Power Unit Based on Dynamic Combined Cost Map and Particle Swarm Optimization. *IEEE Trans. Power Electron.* **2015**, *30*, 7038–7050. [CrossRef]
13. Tang, D.; Zhang, Z.; Hua, L.; Pan, J.; Xiao, Y. Prediction of cold start emissions for hybrid electric vehicles based on genetic algorithms and neural networks. *J. Clean. Prod.* **2023**, *420*, 138403. [CrossRef]
14. Zeng, Y.P. Parameter optimization of plug-in hybrid electric vehicle based on quantum genetic algorithm. *Clust. Comput.* **2019**, *22*, 14835–14843. [CrossRef]
15. Maino, C.; Misul, D.; Musa, A.; Spessa, E. Optimal mesh discretization of the dynamic programming for hybrid electric vehicles. *Appl. Energy* **2021**, *292*, 116920. [CrossRef]

16. Yang, Y.; Pei, H.; Hu, X.; Liu, Y.; Hou, C.; Cao, D. Fuel economy optimization of power split hybrid vehicles: A rapid dynamic programming approach. *Energy* **2019**, *166*, 929–938. [CrossRef]
17. Vu, T.M.; Moezzi, R.; Cyrus, J.; Hlava, J.; Petru, M. Parallel Hybrid Electric Vehicle Modelling and Model Predictive Control. *Appl. Sci.* **2021**, *11*, 10668. [CrossRef]
18. Pozzato, G.; Müller, M.; Formentin, S.; Savaresi, S.M. Economic MPC for online least costly energy management of hybrid electric vehicles. *Control Eng. Pract.* **2020**, *102*, 104534. [CrossRef]
19. Boujelben, M.; Trigui, R. Optimal Power Control for a Variable-Speed Generator Integrated in Series Hybrid Vehicle. *IEEE Trans. Transp. Electrif.* **2022**, *8*, 1302–1312. [CrossRef]
20. Gao, A.; Fu, Z.; Tao, F. Dynamic Coordinated Control Based on Sliding Mode Controller During Mode Switching with ICE Starting for an HEV. *IEEE Access* **2020**, *8*, 60428–60443. [CrossRef]
21. Zhao, J.; Ma, Y.; Zhang, Z.; Wang, S.W.; Wang, S. Optimization and matching for range-extenders of electric vehicles with artificial neural network and genetic algorithm. *Energy Convers. Manag.* **2019**, *184*, 709–725. [CrossRef]
22. Fu, Z.; Su, P.; Song, S.; Tao, F. Mode Transition Coordination Control for PHEV Based on Cascade Predictive Method. *IEEE Access* **2019**, *7*, 138403–138414. [CrossRef]
23. Barsali, S.; Miulli, C.; Possenti, A. A Control Strategy to Minimize Fuel Consumption of Series Hybrid Electric Vehicles. *IEEE Trans. Energy Convers.* **2004**, *19*, 187–195. [CrossRef]
24. Darwich, I.; Lachhab, I.; Krichen, L. Improved electric Vehicle Performance Using on line PSO approach. In Proceedings of the 19th International Conference on Sciences and Techniques of Automatic Control and Computer Engineering (STA), Sousse, Tunisia, 24–26 March 2019; pp. 134–138.
25. Rajput, S.; Moulik, B.; Singh, H.P. Adaptive Power Management of Hybrid Electric Vehicle with Neural Based PID Controller. In Proceedings of the 4th IEEE Uttar Pradesh Section International Conference on Electrical, Computer and Electronics (UPCON), Mathura, India, 26–28 October 2017; pp. 505–511.
26. Demirci, M.; Biliroglu, A.Ö.; Gökasan, M.; Bogosyan, S. Sliding mode optimum control for APU of series hybrid electric vehicles. In Proceedings of the 2010 IEEE International Symposium on Industrial Electronics, Bari, Italy, 4–7 July 2010; pp. 340–345.
27. Ouddah, N.; Adouane, L. Hybrid Energy Management Strategy Based on Fuzzy Logic and Optimal Control for Tri-Actuated Powertrain System. *IEEE Trans. Veh. Technol.* **2019**, *68*, 5343–5355. [CrossRef]
28. Chamsai, T.; Jirawattana, P.; Radpukdee, T. Robust Adaptive PID Controller for a Class of Uncertain Nonlinear Systems: An Application for Speed Tracking Control of an SI Engine. *Math. Probl. Eng.* **2015**, *2015*, 510738. [CrossRef]
29. Kang, M.; Shen, T. Model predictive control of gasoline engines with nonlinear feedback linearized model. In Proceedings of the 2014 18th International Conference on System Theory, Control and Computing (ICSTCC), Sinaia, Romania, 17–19 October 2014; pp. 369–374.
30. Huang, Y.; Jiang, F.; Xie, H. Adaptive hierarchical energy management design for a novel hybrid powertrain of concrete truck mixers. *J. Power Sources* **2021**, *509*, 230325. [CrossRef]
31. Huang, Y.; Wang, S.; Li, K.; Fan, Z.; Xie, H.; Jiang, F. Multi-parameter adaptive online energy management strategy for concrete truck mixers with a novel hybrid powertrain considering vehicle mass. *Energy* **2023**, *277*, 127700. [CrossRef]
32. Mahanpoor, M.; Monajjem, S.; Balali, V. An optimization model for synchronous road geometric and pavement enhancements. *J. Traffic Transp. Eng. (Engl. Ed.)* **2021**, *8*, 421–438. [CrossRef]
33. Hasanoglu, S.M.; Dolen, M. Multi-objective feasibility enhanced particle swarm optimization. *Eng. Optim.* **2018**, *50*, 2013–2037. [CrossRef]
34. Vladov, S.; Scislo, L.; Sokurenko, V.; Muzychuk, O.; Vysotska, V.; Sachenko, A.; Yurko, A. Helicopter Turboshaft Engines' Gas Generator Rotor R.P.M. Neuro-Fuzzy On-Board Controller Development. *Energies* **2024**, *17*, 4033. [CrossRef]